


Contribution of vibrational overtone excitations to positron annihilation rates for benzene and naphthalene

Ryusei Iida, Haruya Suzuki, and Toshiyuki Takayanagi 

Department of Chemistry, Saitama University, Shimo-Okubo 255, Sakura-ku, Saitama, Saitama 338–8570, Japan

Masanori Tachikawa*

Graduate School of Nanobioscience, Yokohama City University, 22-2 Seto, Kanazawa-ku, Yokohama, Kanagawa 236-0027, Japan



(Received 9 August 2021; revised 9 November 2021; accepted 30 November 2021; published 14 December 2021)

Positron-electron annihilation spectra of benzene, deuterated benzene, and naphthalene were theoretically calculated as a function of positron collision energy using Feshbach vibrational resonance energies and widths, which can be obtained from the correlation-polarization-potential model. We found that the contribution of overtone excitations to the annihilation spectrum becomes large for the vibrational mode, where structural deformation along the corresponding vibrational coordinate significantly changes the positron binding energy and polarizability. This behavior occurs for the ν_2 vibrational mode in benzene and deuterated benzene, corresponding to symmetric ring stretching. Since the incoming positron is dominantly attracted by the π electrons of benzene, we conclude that the ring stretching vibration largely affects the π -electron density of the benzene ring.

DOI: [10.1103/PhysRevA.104.062807](https://doi.org/10.1103/PhysRevA.104.062807)

I. INTRODUCTION

High-resolution low-energy positron beam techniques, developed by Surko's group over the past two decades, have established that many (over 90) polyatomic molecules have sizable positive positron binding energies [1–13]. Their extensive experimental studies have shown that the magnitude of the positron binding energy is generally correlated with molecular properties, including dipole polarizability, permanent dipole moment, and the number of π bonds [8]. In their studies, the positron binding energy of a molecule is indirectly obtained from the positron-electron annihilation rate spectrum measured as a function of positron collision energy, which frequently shows enhanced resonance peaks. The resonance energy E_{res} can be simply expressed by $E_{\text{res}} = \hbar\omega_v - E_b$, where ω_v and E_b are the vibrational frequency of a v th mode and the positron binding energy of the target molecule, respectively. In general, strongly enhanced resonances occur for dipole-allowed fundamental vibrational excitation, so the resonance enhanced positron annihilation spectrum of the molecule is very similar in shape to the corresponding infrared vibrational absorption spectrum but with an energy shift corresponding to E_b . Thus, a colliding positron with the resonance energy can temporarily excite the dipole-allowed vibrational mode via the vibrational Feshbach resonance mechanism [1]. The vibrational Feshbach mechanism of the resonant positron annihilation in a molecule is schematically shown in Fig. 1. Only the vibrationally excited states of the positron-bound molecule, with energies above the vibrational ground state of the neutral molecule, can contribute to the annihilation spec-

trum. Based on the Feshbach resonance mechanism, Gribakin and Lee developed a very useful theory for analyzing the measured annihilation spectrum in a simple way [14,15]. The above-mentioned experimental and theoretical studies have revealed that molecular vibrations play an essential role in the positron binding phenomenon in molecules [1,14–18].

It was recently pointed out that the theory of Gribakin and Lee cannot explain some resonance peaks observed for large polyatomic molecules [13,19,20]. Gribakin *et al.* therefore extended the original theory of Gribakin and Lee, which considered only fundamental vibrational excitations, to include the effect of mode-mode coupling and multi-quantum excitations [19]. They demonstrated that this extension works well; however, nondipole transitions are not yet taken into account in their theory. Indeed, experiments suggest that infrared-inactive vibrational excitations can contribute to the positron annihilation spectra measured for *trans*-dichloroethylene and tetrachloroethylene [13]. In addition, a more recent study by Ghosh *et al.* [20] showed that dipole-forbidden overtone vibrations can contribute to the annihilation spectra of cyclopentane, cyclooctane, and heptane. These new experimental studies thus demonstrate that a more reliable theory is required that can describe equally both dipole-allowed and dipole-forbidden transitions in the calculated positron annihilation spectrum.

Our research group has been developing a density-functional theory (DFT)-based approach, where the positron-molecule interaction is described using a correlation-polarization potential (CPP). Our aim is to understand the positron binding phenomena in polyatomic molecules using a theoretical perspective [21–24]. The important advantage of this DFT-CPP approach is that one can calculate the positron-molecule interaction potential as a function of the nuclear

*Corresponding author: tako@mail.saitama-u.ac.jp

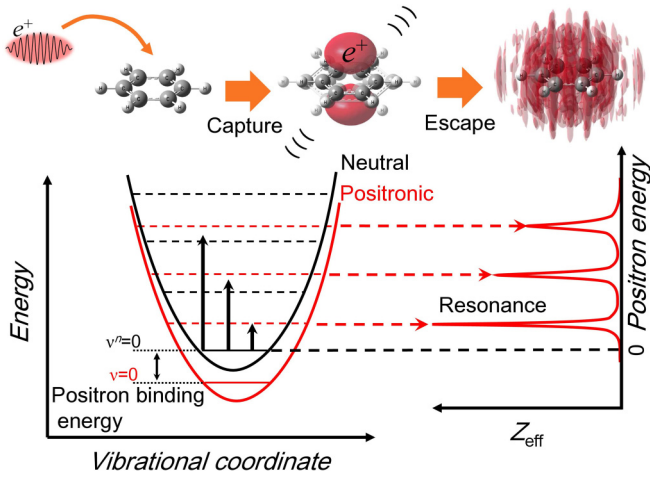


FIG. 1. Schematic representation of the positron-electron annihilation phenomenon through the vibrational Feshbach resonance mechanism for positron-molecule collision. The left panel shows schematic potential-energy curves for the neutral and positronic molecule as a function of vibrational coordinates. When the initial neutral molecule is assumed to be in the vibrational ground state, the positron is resonantly captured into vibrational excited states of the positron-bound molecule, followed by annihilation or escape from the molecule.

coordinates of the molecule. This enables calculations of the coupling between incoming and outgoing positron motion in the scattering state and molecular vibrational motion, which determines the vibrational Feshbach resonance widths. We previously employed the DFT-CPP approach to calculate the resonance-dominated positron annihilation spectra of several molecules and obtained good agreement between theory and experiment [23,24]. In the present paper, using DFT-CPP theory we discuss the importance of overtone excitations for infrared-inactive vibrational modes in the positron annihilation spectra for benzene, deuterated benzene, and naphthalene. It is generally known, in molecular vibrational spectroscopy, that the contribution of overtone excitation cannot be understood by simple harmonic selection rules and that the overtone intensity comes from a combination of mechanical anharmonicity (the potential is not simply a harmonic oscillator) and electrical anharmonicity (the dipole moment is not a linear function of bond displacement) [25,26]. In the case of positron scattering, there should exist an additional factor that can influence overtone intensities. The neutral and positronic potential-energy curves are generally not parallel as a function of the vibrational coordinate since the positron binding energy depends on the structural displacement [23] and it is expected that this factor can also affect the overtone intensities. This is in high contrast with the fundamental vibrational transition case where the resonance intensities in the positron annihilation spectrum can be understood in terms of infrared absorption intensities for a molecule [14,15]. Thus, it is important to numerically calculate the overtone intensity in the positron annihilation spectrum to understand the detailed mechanisms on the contribution of overtone excitations in position scattering.

II. THEORY

We here only briefly describe our computational method for calculating the annihilation spectrum (Z_{eff}) as the method is described in detail in Refs. [23,24]. We assume that positron annihilation occurs exclusively through the vibrational Feshbach resonance mechanism and thus can be described in the usual Breit-Wigner form [14,15]:

$$Z_{\text{eff}}(E) = \frac{\pi}{k} \rho_{ep} \sum_v \frac{g_v \Gamma_v^e}{(E - E_v)^2 + \Gamma_v^2/4}, \quad (1)$$

where E_v , Γ_v^e , Γ_v , and g_v are the resonance energy, elastic resonance capture width, total width, and degeneracy of the vibrational state, respectively, with v being a vibrational quantum number. In addition, E , k , and ρ_{ep} are positron energy, positron momentum (with $E = k^2/2$), and positron-electron contact density, respectively. The positron capture width Γ_v^e (in atomic unit) was calculated using Fermi's "golden rule" approximation [27–29] as

$$\Gamma_v^e = 2\pi |\langle \psi_f(E_v, r; Q) | V_i(r; Q) | \psi_i(r; Q) \rangle|^2, \quad (2)$$

where the resonance energy is taken to be a specific vibrational energy level of the target molecule (E_v , with v denoting the vibrational quantum number). The bound-state solution of the Schrödinger equation for the positron-molecule system provides the positron binding energy and the positron wave function ψ_i . Also, we can obtain the positron scattering wave function ψ_f at a specific collision energy from the same Schrödinger equation but with scattering boundary conditions. The interaction potential V_i can be approximated by the first-order Taylor series around the equilibrium nuclear coordinate, Q_e , and the resonance width can be therefore written as [23,24]

$$\Gamma_v^e(E) = 2\pi |\langle \chi_0(Q) | Q - Q_e | \chi_v^p(Q) \rangle|^2 \times |\langle \phi_c(E, r; Q_e) | \frac{\partial}{\partial Q} V(r, Q) |_{Q_e} | \phi_b(r; Q_e) \rangle|^2, \quad (3)$$

where $\chi_v^p(Q)$ and $\chi_{v=0}(Q)$ are the vibrationally excited wave function on the positronic potential-energy surface and the vibrational ground-state wave function on the neutral potential-energy surface, respectively. ϕ_b and ϕ_c are the positronic wave functions for the bound and continuum states, respectively. For example, if $\chi_v^p(Q)$ and $\chi_0(Q)$ can be described by the same harmonic potentials, the magnitude of overtone intensity for $v = 2$ should be zero because the first factor corresponding to the vibrational wave functions is zero. Also, it is worth mentioning that the second factor containing the first derivative term does not depend on the vibrational states in our approximation.

The resonance width was calculated numerically using the time-dependent "golden rule" approach, which is more efficient than the time-independent approach [30–33]. The Schrödinger equation for positron motion in the molecule can be easily given once the positron-molecule interaction is provided. We used the DFT-CPP model originally applied to extensive positron-molecule scattering studies performed by Gianturco and other researchers [34–47]. In the DFT-CPP method, the short-range potential is approximated by a local positron-electron potential derived from the local electron

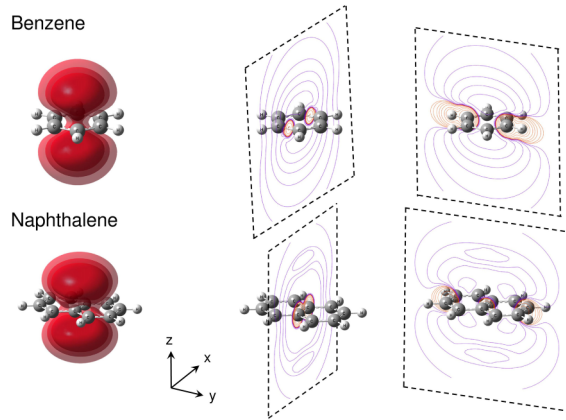


FIG. 2. Three-dimensional plots of the positron densities (left panels) for benzene and naphthalene calculated using the CPP model with the GGA functional ($\beta = 0.075$ and 0.19 for benzene and naphthalene, respectively). The positron densities are indicated by three surface contour values, which correspond to 0.0008 , 0.0006 , and $0.0004 e^+/a_0^3$. Positron-molecule interaction potentials (right panels) projected on the two planes ($x, y = 0, z$) and ($x = 0, y, z$). Positive (repulsive) and negative (attractive) energy contours are indicated with red and purple contour lines, respectively.

density based on the DFT framework, whereas the long-range attractive potential is approximated by dipole polarizabilities. We found that the calculated positron binding energies can be improved by introducing the generalized gradient approximation (GGA) [48,49] into the DFT-based potential. The explicit equations are given in Ref. [21].

The positron-electron contact density was calculated using the following equation:

$$\rho_{ep} = \int \gamma(r) |\psi_i(r)|^2 \rho(r) dr, \quad (4)$$

where r is the positron coordinate and ρ is the electron density at the positron position. $\gamma(r)$ is an enhancement factor that accounts for the short-range positron-electron Coulomb attraction, and we employed the following expression proposed by Barbiellini *et al.* [48]:

$$\gamma(r) = 1 + (1.23r_s - 0.0742r_s^2 + \frac{1}{6}r_s^3) \times \exp[-\beta |\nabla \rho|^2 / (\rho q_{TF})^2], \quad (5)$$

where r_s is the electron density parameter with $r_s = (3/4\pi\rho)^{1/3}$ and q_{TF} is the local Thomas-Fermi screening length. β is the parameter controlling the gradient contribution in the positron-electron interaction potential. Here, β is assumed to be an adjustable parameter and was optimized so that the calculated positron binding energy reproduces the measured positron binding energy of the molecule.

The electron densities for benzene and naphthalene were calculated using the Perdew-Burke-Ernzerhof exchange-correlation functional combined with aug-cc-pVDZ basis sets using the GAUSSIAN09 quantum chemistry calculation code [50]. The combination of this DFT exchange-correlation functional and basis set, including diffuse functions, was chosen from extensive benchmarking calculations, where we confirmed that this combination yields reliable vibrational

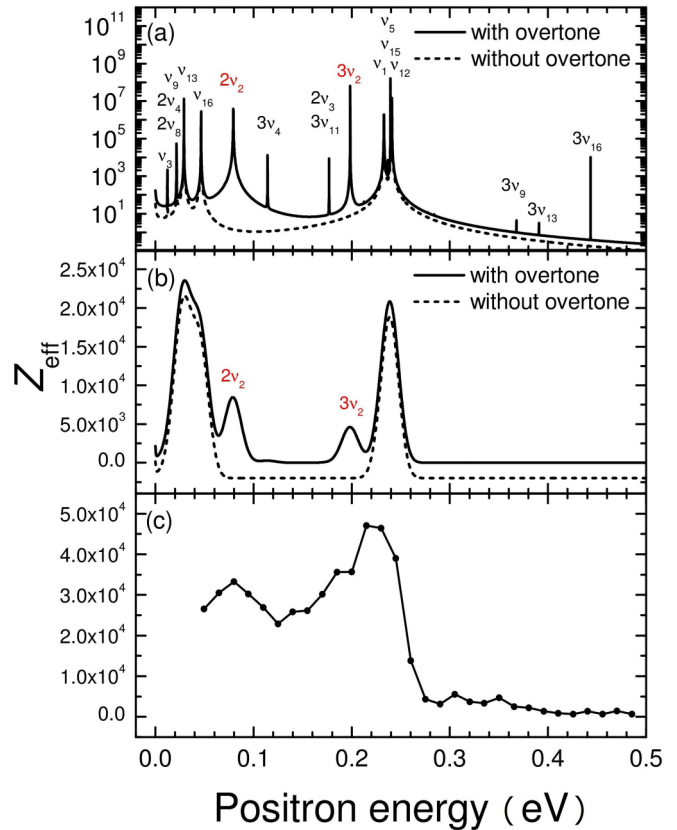


FIG. 3. Comparison of the experimental and theoretical annihilation spectra of benzene. Panel (a) shows the calculated spectra with and without contribution of overtone excitations (on a logarithmic scale). Panel (b) shows the calculated spectra convoluted with a Gaussian function of 20 meV width (on a linear scale). The solid black and dotted lines indicate the results with and without contribution of overtone excitations, respectively. Note that the spectra calculated without the contribution of overtone excitations are vertically shifted by -2000 . Panel (c) shows the experimental spectrum taken from Ref. [4].

frequencies and polarizability tensors. The positron wave functions were obtained by numerically solving the positron Schrödinger equations with the Cartesian particle-in-a-box discrete-variable-representation method [51]. We applied a cutoff energy parameter of 30 hartrees to the total positron-molecule potential to avoid divergent Coulomb repulsion from positive nuclei. We employed $(256)^3$ grid points in the range of $-L/2 \leq (x, y, z) \leq L/2$, where the coordinate origin is taken as the target molecule's center of mass. L is the box size and was taken to be $70 a_0$. We used the direct relaxation method [52], where the initial trial wave function is propagated in imaginary time through the time-dependent Schrödinger equation, to obtain the positronic bound state. Similar to the bound-state case, we solved the standard time-dependent Schrödinger equations using the well-known fast Fourier-transform algorithm combined with the split-operator method [52]. In this paper, we employ normal-mode coordinates to describe the molecular structure. We solved the positron bound-state problem using the discrete variable representation (DVR) method at a chosen point along each normal-mode coordinate. This provides the

TABLE I. Resonance energies and widths of benzene (C_6H_6 , D_{6h}) for each vibrational state calculated using the CPP model with the GGA functional. The characteristics of each vibrational mode are indicated. Resonance with a small width ($\Gamma < 10^{-10}$) is ignored.

Mode (sym.)	Resonance energy (eV)			Resonance width (a.u.) ^a			Infrared or Raman Activity	Vibration type
	Fundamental	First overtone	Second overtone	Fundamental	First overtone	Second overtone		
$\nu_4(a_u)$			0.114			1.26 (−9)	Active or inactive	CH bend
$\nu_{11}(e_{1g})$		0.065	0.177			1.33 (−10)	Inactive or active	CH bend
$\nu_2(a_{1g})$		0.079	0.197		5.16 (−6)	1.90 (−7)	Inactive or active	Ring stretch
$\nu_3(a_{2g})$	0.012	0.176	0.341	1.57 (−10)			Inactive or active	CH bend
$\nu_9(b_{2u})$	0.021		0.368	2.26 (−9)			Active or inactive	Ring stretch
$\nu_{13}(e_{1u})$	0.029		0.391	8.27 (−8)			Active or inactive	Ring stretch + deform
$\nu_{16}(e_{2g})$	0.046	0.244	0.443	8.92 (−8)			Inactive or active	Ring stretch
$\nu_5(b_{1u})$	0.237		1.022	2.15 (−10)			Active or inactive	CH stretch
$\nu_{15}(e_{2g})$	0.239		1.033	1.19 (−7)			Inactive or active	CH stretch
$\nu_{12}(e_{1u})$	0.241		1.038	1.71 (−6)			Active or inactive	CH stretch
$\nu_1(a_{1g})$	0.233	0.615	0.996	2.47 (−6)	1.31 (−8)		Inactive or active	CH stretch

^aThe notation $a(b)$ means $a \times 10^b$.

one-dimensional potential-energy curve for a positron bound molecule as a function of each normal mode. By solving the one-dimensional eigenvalue problem, we can easily obtain the vibrational energy levels which correspond to the resonance positions for positron collision.

III. RESULTS AND DISCUSSION

To calculate the annihilation spectra for benzene and naphthalene, we must first determine the appropriate gradient contribution parameter β in Eq. (5). In this paper, the β values for benzene and naphthalene were independently optimized so that the calculated positron binding energies for benzene and naphthalene at their equilibrium structures nearly reproduce the measured positron binding energies. The β values were optimized to be 0.075 for benzene and 0.19 for naphthalene. The positron binding energies for benzene and naphthalene calculated with these β values are 150.4 and 300.4 meV, respectively, and are comparable to the corresponding experimental values, 150 and 300 meV [4,5]. The previous experimental study showed no isotope effect in the positron binding energy for benzene. These β values are not universal since the optimal value significantly depends on the level of quantum chemistry used. In Fig. 2, we present the calculated positron densities and positron-molecule interaction potentials; the positron is attracted by the π electrons for both benzene and naphthalene. The importance of the π electrons in positron binding was observed in our previous study on chloroethene molecules [24]. Such attractive interaction between the positron and π electrons can also be understood from plots of the interaction potentials projected onto two molecular planes, presented in Fig. 2.

Next, we discuss the contributions of overtone excitations to the calculated positron-electron annihilation spectrum. Figure 3(a) shows the calculated spectra without energy convolution for benzene: we present the annihilation spectra with and without the contribution of overtone excitations. The calculated resonance energies and widths are summarized in Table I, along with the vibrational mode assignment taken from NIST Chemistry WebBook [53]. Notice that some vi-

brational modes with low frequencies do not contribute to the positron annihilation spectrum, for which the corresponding excitation energy is smaller than the positron binding energy (see Fig. 1). Also, in Table I, the resonance with a very small width ($\Gamma < 10^{-10}$ a.u.) is ignored since such a resonance does not contribute to the convoluted spectrum (all the numerical results are presented in the Supplemental Material [54]). The calculated spectra convoluted with a Gaussian distribution of 20-meV width are shown in Fig. 3(b) to compare with the experimental spectrum shown in Fig. 3(c). The dominant peaks around $E = 0.23$ eV in the convoluted spectra shown in Fig. 3(b) are associated with an infrared active mode (ν_{12} mode), followed by the contribution of the ν_1 mode. The ν_1 vibrational mode with a_{1g} symmetry is Raman active and infrared inactive. The large contribution of this mode occurs through the $\partial V/\partial Q$ interaction term in Eq. (3), where the dominant interaction comes from the change in dipole polarizability along the normal-mode coordinate. We previously discussed this behavior in detail [23].

From the comparison between the calculated spectra with and without contribution of overtone excitations, it is interesting to note that the overtone contribution of the ν_2 vibrational mode, which corresponds to symmetric ring stretching with a_{1g} symmetry (Raman active or infrared inactive) under the D_{6h} point group, is relatively large. The resonance energies with two- and three-quanta overtone excitations can be seen at $E = 0.079$ and 0.197 eV, respectively (see also Table I). More interestingly, these overtone excitation peaks overlap with the shoulders of the fundamental transition peaks in the experimental spectrum, suggesting the importance of these overtone peaks. Thus, inclusion of the overtone excitation contribution provides better agreement with the measured spectrum, although the energy resolution of the measured spectrum may still be too low to support a concrete conclusion.

To further understand the reason for the large contribution of the ν_2 mode, in Fig. 4 we show the potential-energy curves of the neutral and positron-bound benzene molecule as a function of the ν_2 normal-mode coordinate, along with the positron binding energy, dipole moment, and isotropic polarizability. As mentioned above, the ν_2 normal mode is

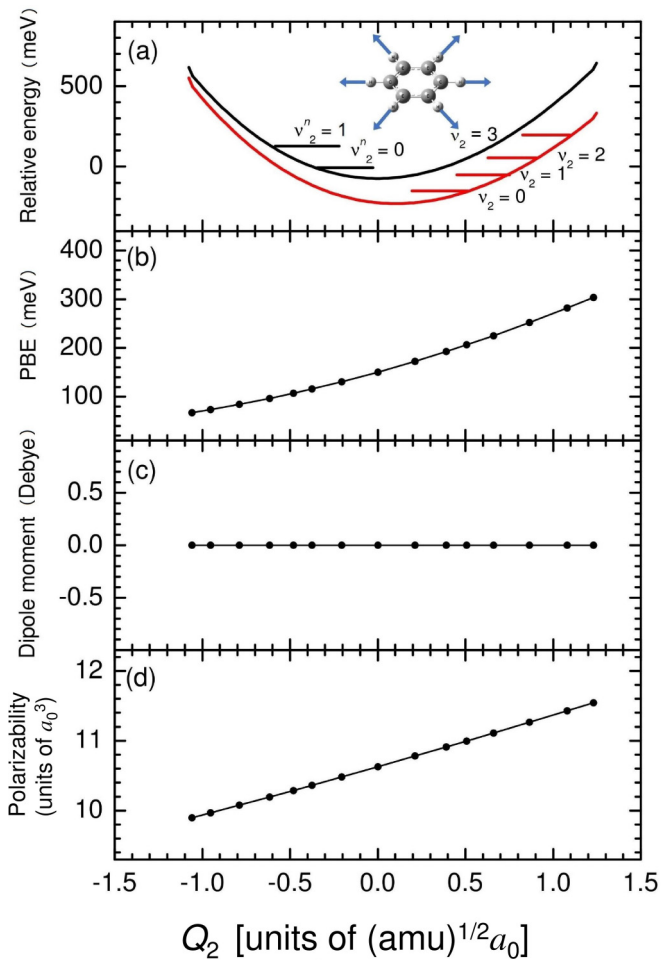


FIG. 4. Potential-energy curves of neutral and positronic molecules (a), positron binding energy (b), dipole moment (c), and isotropic polarizability (d) for benzene (C_6H_6) as a function of the normal-mode coordinate of the ν_2 ring stretching mode. Vibrational energy levels obtained by solving the one-dimensional Schrödinger equation are also shown, where ν_i and ν_i^n are the vibrational quantum numbers for positronic and neutral molecules, respectively.

associated with symmetric ring stretching, and a change in this mode affects the size of the benzene ring in which its D_{6h} symmetry can be maintained. The positron binding energy linearly increases as the normal-mode coordinate increases as shown in Fig. 4(b), and this increase is highly correlated with the magnitude of the isotropic dipole polarizability shown in Fig. 4(d). This leads to deviation of the positron-bound potential-energy curve along the ν_2 normal-mode coordinate from the neutral potential-energy curve, and thus the two potential-energy curves are not parallel along the normal-mode coordinate, as shown in Fig. 4(a). This behavior leads to a nonzero overlap between the ground vibrational wave function in the neutral state and the vibrationally excited-state wave function in the positronic state and to the increase in the first factor in Eq. (3). In addition, the large contribution of the ν_2 ring stretch motion in positron binding for benzene can qualitatively be understood from the positron density shown in Fig. 2. As mentioned previously, the incoming positron is largely attracted by the π electrons in benzene. Nuclear

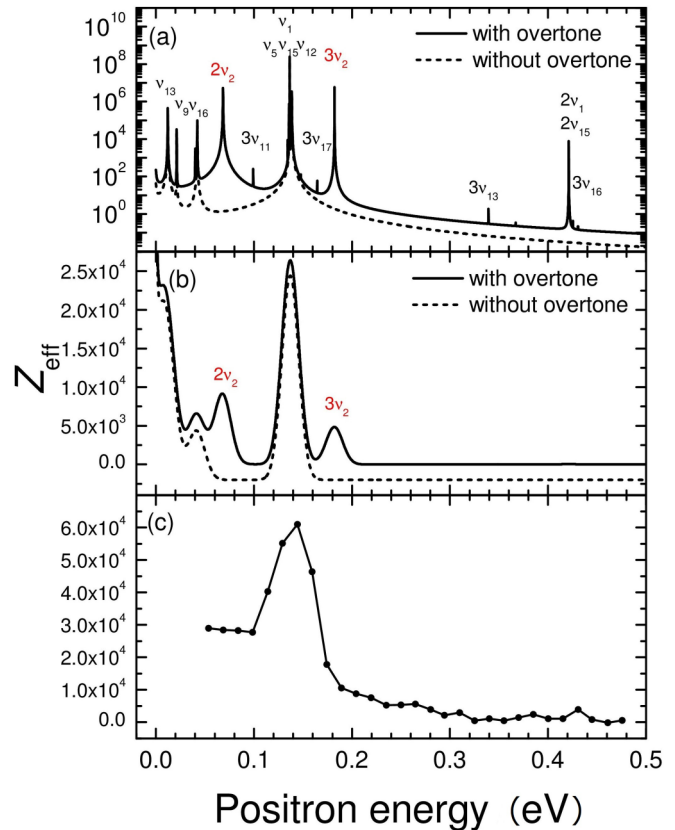


FIG. 5. Comparison of the experimental and theoretical annihilation spectra of deuterated benzene. Panel (a) shows the calculated spectra with and without contribution of overtone excitations (on a logarithmic scale). Panel (b) shows the calculated spectra convoluted with a Gaussian function of 20-meV width (on a linear scale). The solid black and dotted lines indicate the results with and without contribution of overtone excitations, respectively. Note that the spectra calculated without the contribution of overtone excitations are vertically shifted by -2000 . Panel (c) shows the experimental spectrum taken from Ref. [4].

motion along the ν_2 normal coordinate significantly affects π -electron density and thus dipole polarizability through the change in ring size.

As mentioned previously, in this paper, an adjustable gradient parameter β has been optimized at 0.075 for benzene so as to reproduce the measured positron binding energy because the positron binding energy determines the vibrational resonance positions in the positron annihilation spectrum. It is worth mentioning that β was set to 0.22 in Ref. [48] while β was set to 0.05 in Ref. [49] from the comparison to experiment. Thus, the present value is found to be reasonably in the range of these two studies. However, it may be important to understand how the magnitude of the gradient parameter β affects the calculated resonance properties. We have therefore calculated the resonance properties for the ν_1 and ν_2 vibrational modes of benzene with $\beta = 0.06$ and 0.09 (corresponding to 0.8β and 1.2β , respectively). Notice that the ν_1 mode gives the largest width for fundamental excitation while the ν_2 mode gives largest resonance widths for overtone excitation. The result of this calculation is presented in the Supplemental Material [54]. The most important finding of

TABLE II. Resonance energies and widths of deuterated benzene (C_6D_6 , D_{6h}) for each vibrational state calculated using the CPP model with the GGA functional. The characteristics of each vibrational mode are indicated. Resonance with a small width ($\Gamma < 10^{-10}$) is ignored.

Mode (sym.)	Resonance energy (eV) Fundamental	First overtone	Second overtone	Resonance width (a.u.) ^a Fundamental	First overtone	Second overtone	Infrared or Raman Activity	Vibration type
$\nu_4(a_{2u})$			0.040			3.91 (-10)	Active or inactive	CD bend
$\nu_2(a_{1g})$		0.068	0.182		5.15 (-6)	2.00 (-7)	Inactive or active	Ring stretch
$\nu_{13}(e_{1u})$	0.012	0.175	0.339	2.88 (-8)			Active or inactive	Ring stretch + deform
$\nu_9(b_{2u})$	0.021		0.367	1.38 (-9)			Active or inactive	Ring stretch
$\nu_{16}(e_{2g})$	0.042		0.431	1.16 (-8)			Inactive or active	Ring stretch
$\nu_5(b_{1u})$	0.134		0.710	2.18 (-10)			Active or inactive	CD stretch
$\nu_{15}(e_{2g})$	0.136	0.426	0.718	9.01 (-8)			Inactive or active	CD stretch
$\nu_{12}(e_{1u})$	0.139	0.430	0.725	7.97 (-7)			Active or inactive	CD stretch
$\nu_1(a_{1g})$	0.136	0.421	0.707	8.04 (-8)	3.67 (-10)		Inactive or active	CD stretch

^aThe notation $a(b)$ means $a \times 10^b$.

this calculation is that the resonance widths for fundamental transitions do not significantly depend on the value of β . The second factor of the resonance width in Eq. (3) is found to only weakly depend on β . In the case of overtone transitions, the overall resonance widths are found to also weakly depend on β ; however, the dependence comes from the first factor in Eq. (3), which is corresponding to the vibrational wavefunction contribution and determines the resonance width. These results suggest that the optimization of the β value is a reasonable strategy since the change in β does not largely affect the annihilation spectral shape which is associated with fundamental transitions. Nevertheless, it may be ideal to calculate the positron annihilation spectrum with a universal β value. In this sense, it is worth mentioning that the parameter-free equation for calculating the electron-positron interaction has recently been proposed by Barbiellini and Kuriplach [55].

Figure 5 shows annihilation spectra similar to Fig. 3 but for deuterated benzene, C_6D_6 . Figure 6 shows the potential-energy curves, positron binding energy, dipole moment, and isotropic polarizability as a function of the normal-mode coordinate, similar to Fig. 4 but for C_6D_6 . The calculated resonance energies and widths are summarized in Table II. As in the case of C_6H_6 , the contribution of overtone excitations of the ν_2 mode is important in the calculated spectrum [see Fig. 5(b)], and the resonance energies with two- and three-quanta excitations are seen at $E = 0.068$ and 0.182 eV, respectively. However, the calculated and experimental spectra agree less well compared with those of benzene, highlighting the need to experimentally measure the annihilation spectrum at higher energy resolution. Also, from a theoretical viewpoint, there is the possibility that higher-order terms [see Eq. (3)] and mode-mode couplings [19] should be included to obtain more accurate overtone intensities. This point should be studied in the future.

Finally, we present the results for naphthalene as another example of a molecule with an aromatic ring with π electrons. Figures 7(a) and 7(b) show the calculated spectra without and with energy convolution for naphthalene; the two annihilation spectra with and without the contributions of overtone excitations are shown. The calculated resonance energies and widths are summarized in Table III, along with the vibrational mode

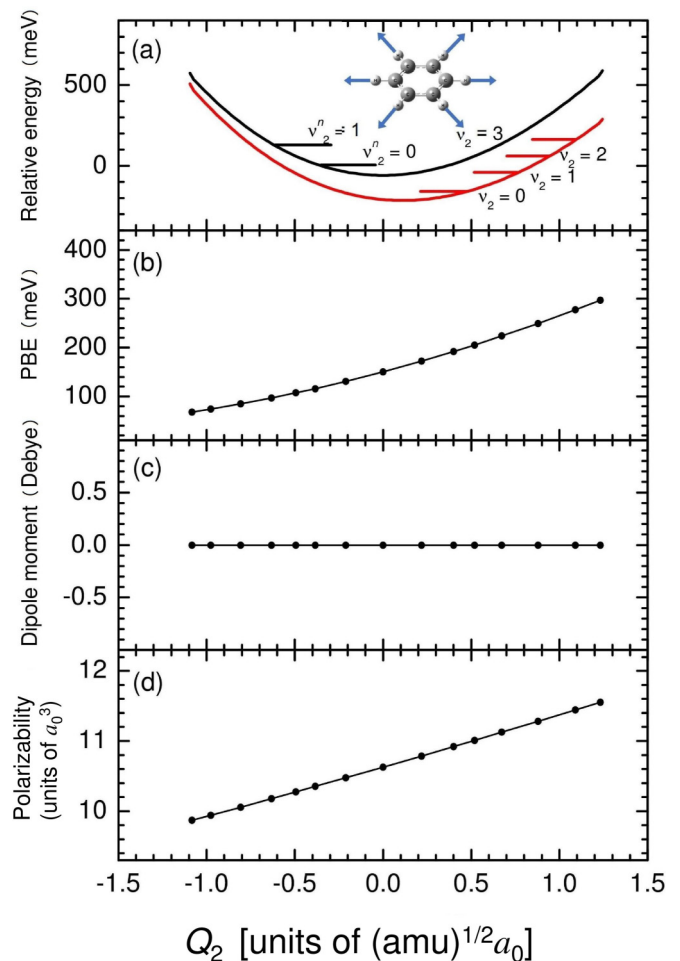


FIG. 6. Potential-energy curves of neutral and positronic molecules (a), positron binding energy (b), dipole moment (c), and isotropic polarizability (d) for deuterated benzene (C_6D_6) as a function of the normal-mode coordinate of the ν_2 ring stretching mode. Vibrational energy levels obtained by solving the one-dimensional Schrödinger equation are also shown, where ν_i and ν_i^n are the vibrational quantum numbers for positronic and neutral molecules, respectively.

TABLE III. Resonance energies and widths of naphthalene ($C_{10}H_8$, D_{2h}) for each vibrational state calculated using the CPP model with the GGA functional. The characteristics of each vibrational mode are indicated. Resonance with a small width ($\Gamma < 10^{-10}$) is ignored.

Mode (sym.)	Resonance energy (eV) Fundamental	First overtone	Second overtone	Resonance width (a.u.) ^a Fundamental	First overtone	Second overtone	Infrared or Raman Activity	Vibration type
$v_{45}(b_{3u})$			0.055				Active or inactive	CH bend
$v_5(a_g)$		0.048	0.223		9.44 (-10)		Inactive or active	CC stretch
$v_{38}(b_{3g})$	0.087	0.476	0.869	3.21 (-9)			Inactive or active	CH stretch
$v_{18}(b_{1u})$	0.087	0.476	0.869	5.51 (-7)			Active or inactive	CH stretch
$v_{30}(b_{2u})$	0.088	0.479	0.876	5.74 (-9)			Active or inactive	CH stretch
$v_2(b_g)$	0.083	0.465	0.847	1.30 (-7)	1.08 (-9)		Inactive or active	CH stretch
$v_{37}(b_{3g})$	0.089	0.481	0.877	5.41 (-8)			Inactive or active	CH stretch
$v_{17}(b_{1u})$	0.089	0.481	0.876	1.75 (-6)			Active or inactive	CH stretch
$v_{29}(b_{2u})$	0.091	0.486	0.886	3.30 (-7)			Active or inactive	CH stretch
$v_1(a_g)$	0.085	0.469	0.851	5.50 (-8)	5.04 (-10)		Inactive or active	CH stretch

^aThe notation $a(b)$ means $a \times 10^b$.

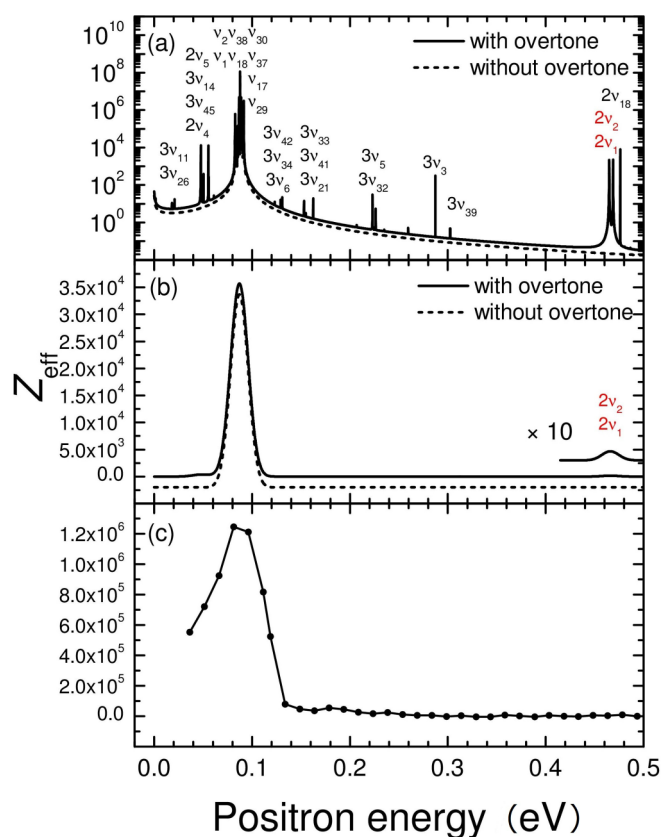


FIG. 7. Comparison of the experimental and theoretical annihilation spectra of naphthalene. Panel (a) shows the calculated spectra with and without contribution of overtone excitations (on a logarithmic scale). Panel (b) shows the calculated spectra convoluted with a Gaussian function of 20 meV width (on a linear scale). The solid black and dotted lines indicate the results with and without contribution of overtone excitations, respectively. Note that the spectra calculated without the contribution of overtone excitations are vertically shifted by -2000 . Panel (c) shows the experimental spectrum taken from Ref. [5].

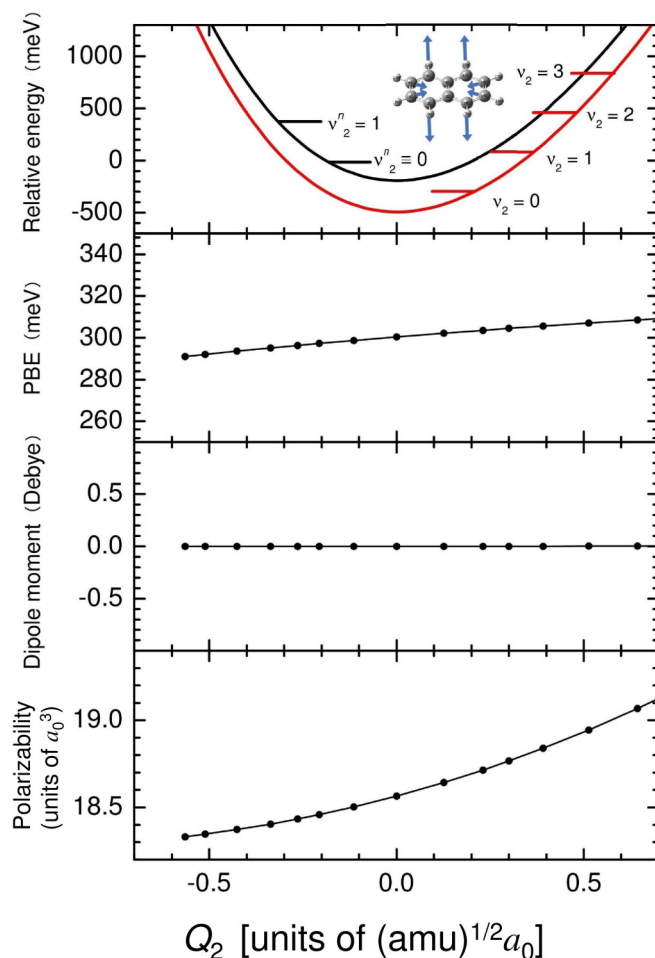


FIG. 8. Potential-energy curves of neutral and positronic molecules (a), positron binding energy (b), dipole moment (c), and isotropic polarizability (d) for naphthalene ($C_{10}H_8$) as a function of the normal-mode coordinate of the v_2 ring stretching mode. Vibrational energy levels obtained by solving the one-dimensional Schrödinger equation are also shown, where v_i and v^n are the vibrational quantum numbers for positronic and neutral molecules, respectively.

assignment taken from NIST CCCBDB [56]. We found that the contribution of overtone excitations in naphthalene is very small. The largest resonance width occurs for the ν_2 mode with the first overtone excitation (two vibrational quanta) at $E = 0.465$ eV in a high-energy region. The small contribution of this overtone excitation to the annihilation spectrum can be understood from the result presented in Fig. 8, where the neutral and positronic potential-energy curves, positron binding energy, dipole moment, and isotropic polarizability are plotted as a function of the normal-mode coordinate. It is seen that isotropic polarizability increases as the normal-mode coordinate increases, and this leads to an increase in the positron binding energy. However, the change in the magnitude of the positron binding energy is very small compared to benzene (see Figs. 4 and 6). In fact, the positron binding energy for benzene increases by ≈ 210 meV from $Q_2 = -1$ to 1. In contrast, the positron binding energy for naphthalene increases by only 15 meV from $Q_2 = -0.5$ to 0.5. Therefore, the neutral and positronic potential-energy curves are nearly parallel for naphthalene, leading to a small overlap between the corresponding two vibrational wave functions. Also, this difference comes from the difference in the vibrational mode character; the Q_2 mode for benzene is corresponding to the ring stretching which can affect the π -electron density, while the Q_2 mode of naphthalene corresponds to the CH stretching which does not largely affect the π -electron density.

IV. CONCLUSIONS

In summary, we have theoretically calculated the positron-annihilation spectra for benzene, deuterated benzene, and naphthalene with the Breit-Wigner formula, assuming the vibrational Feshbach resonance mechanism. Vibrational res-

onance energies and widths were calculated by applying the practical CPP model. In this paper, we mainly discussed the importance of vibrational overtone excitations in the annihilation spectra. We found that the contribution of the overtone excitations becomes large for the vibrational mode, for which a large change in the positron binding energy occurs along the corresponding vibrational coordinate through the change in polarizability. In this case, the neutral and positronic potential-energy curves are not in parallel, leading to a relatively large overlap between the neutral ground vibrational state wave function and the positronic vibrationally excited-state wave function. We found that this behavior occurs for the ν_2 vibrational mode in benzene and deuterated benzene and corresponds to symmetric ring stretching. As a result, the contribution of the ν_2 mode with two- and three-quanta excitations is relatively large in the calculated annihilation spectra. In contrast, in the case of naphthalene, the largest positron binding-energy change occurs for the ν_2 mode but the change in the absolute value is much smaller than that for benzene by a factor of more than 10. In the future, we will extend the present paper to understand the contributions of overtone excitations in the positron annihilation spectra for cyclopentane, cyclooctane, and heptane, for which experimental measurements are available [20]. In addition, the contribution of higher-order terms ignored in the Taylor expansion for calculating the resonance widths and mode-mode couplings should be included in a future study to calculate more accurate positron annihilation spectra.

ACKNOWLEDGMENT

This work was supported by a Grant-in-Aid for Scientific Research from the Ministry of Education, Culture, Sports, Science and Technology of Japan (Grant No. 19K05365).

-
- [1] G. F. Gribakin, J. A. Young, and C. M. Surko, Positron-molecule interactions: Resonant attachment, annihilation, and bound states, *Rev. Mod. Phys.* **82**, 2557 (2010).
 - [2] L. D. Barnes, S. J. Gilbert, and C. M. Surko, Energy-resolved positron annihilation for molecules, *Phys. Rev. A* **67**, 032706 (2003).
 - [3] L. D. Barnes, J. A. Young, and C. M. Surko, Energy-resolved positron annihilation rates for molecules, *Phys. Rev. A* **74**, 012706 (2006).
 - [4] J. A. Young and C. M. Surko, Role of Binding Energy in Feshbach-Resonant Positron-Molecule Annihilation, *Phys. Rev. Lett.* **99**, 133201 (2007).
 - [5] J. A. Young and C. M. Surko, Feshbach-resonance-mediated annihilation in positron interactions with large molecules, *Phys. Rev. A* **77**, 052704 (2008).
 - [6] J. A. Young and C. M. Surko, Feshbach-resonance-mediated positron annihilation in small molecules, *Phys. Rev. A* **78**, 032702 (2008).
 - [7] J. A. Young and C. M. Surko, Positron attachment to molecules, *Phys. Status Solidi C* **6**, 2265 (2009).
 - [8] J. R. Danielson, J. A. Young, and C. M. Surko, Dependence of positron-molecule binding energies on molecular properties, *J. Phys. B* **42**, 235203 (2009).
 - [9] J. R. Danielson, J. J. Gosselin, and C. M. Surko, Dipole Enhancement of Positron Binding to Molecules, *Phys. Rev. Lett.* **104**, 233201 (2010).
 - [10] J. R. Danielson, A. C. L. Jones, M. R. Natisin, and C. M. Surko, Comparisons of Positron and Electron Binding to Molecules, *Phys. Rev. Lett.* **109**, 113201 (2012).
 - [11] J. R. Danielson, A. C. L. Jones, J. J. Gosselin, M. R. Natisin, and C. M. Surko, Interplay between permanent dipole moments and polarizability in positron-molecule binding, *Phys. Rev. A* **85**, 039907(E) (2012).
 - [12] A. C. L. Jones, J. R. Danielson, J. J. Gosselin, M. R. Natisin, and C. M. Surko, Positron binding to alcohol molecules, *New J. Phys.* **14**, 015006 (2012).
 - [13] M. R. Natisin, J. R. Danielson, G. F. Gribakin, A. R. Swann, and C. M. Surko, Vibrational Feshbach Resonances Mediated by Nondipole Positron-Molecule Interactions, *Phys. Rev. Lett.* **119**, 113402 (2017).
 - [14] G. F. Gribakin and C. M. R. Lee, Positron Annihilation in Molecules by Capture into Vibrational Feshbach Resonances of Infrared-Active Modes, *Phys. Rev. Lett.* **97**, 193201 (2006).
 - [15] G. F. Gribakin and C. M. R. Lee, Positron annihilation in large polyatomic molecules: The role of vibrational Feshbach resonances and binding, *Eur. Phys. J. D* **51**, 51 (2009).

- [16] G. F. Gribakin, Theory of positron annihilation on molecules, in *New Directions in Antimatter Chemistry and Physics*, edited by C. M. Surko and F. A. Gianturco (Springer, New York, 2001), p. 413.
- [17] S. d'A. Sanchez, M. A. P. Lima, and M. T. do N. Varela, Feshbach projection operator approach to positron annihilation, *Phys. Rev. A* **80**, 052710 (2009).
- [18] S. d'A. Sanchez, M. A. P. Lima, and M. T. do N. Varela, Multi-mode Vibrational Couplings in Resonant Positron Annihilation, *Phys. Rev. Lett.* **107**, 103201 (2011).
- [19] G. F. Gribakin, J. F. Stanton, J. R. Danielson, M. R. Natisin, and C. M. Surko, Mode coupling and multiquantum vibrational excitations in Feshbach-resonant positron annihilation in molecules, *Phys. Rev. A* **96**, 062709 (2017).
- [20] S. Ghosh, J. R. Danielson, and C. M. Surko, Enhanced Resonant Positron Annihilation due to Nonfundamental Modes in Molecules, *Phys. Rev. Lett.* **125**, 173401 (2020).
- [21] Y. Sugiura, T. Takayanagi, Y. Kita, and M. Tachikawa, Positron binding to hydrocarbon molecules: Calculation using the positron-electron correlation polarization potential, *Eur. Phys. J. D* **73**, 162 (2019).
- [22] Y. Sugiura, H. Suzuki, T. Otomo, T. Miyazaki, T. Takayanagi, and M. Tachikawa, Positron-electron correlation-polarization potential model for positron binding in polyatomic molecules, *J. Comput. Chem.* **41**, 1576 (2020).
- [23] Y. Sugiura, T. Takayanagi, and M. Tachikawa, Theoretical calculation of positron annihilation spectrum using positron-electron correlation-polarization potential, *Int. J. Quantum Chem.* **120**, e26376 (2020).
- [24] H. Suzuki, T. Otomo, R. Iida, Y. Sugiura, T. Takayanagi, and M. Tachikawa, Positron binding in chloroethenes: Modeling positron-electron correlation-polarization potentials for molecular calculations, *Phys. Rev. A* **102**, 052830 (2020).
- [25] K. K. Lehmann and A. M. Smith, Where does overtone intensity come from?, *J. Chem. Phys.* **93**, 6140 (1990).
- [26] D. P. Schofield, J. R. Lane, and H. G. Kjaergaard, Hydrogen bonded OH-stretching vibration in the water dimer, *J. Phys. Chem. A* **111**, 567 (2007).
- [27] J. Ulstrup and J. Jortner, The effects of free energy and solvent on the reaction rates, *J. Chem. Phys.* **63**, 4358 (1975).
- [28] R. A. Marcus and N. Sutin, Electron transfers in chemistry and biology, *Biochim. Biophys. Acta* **811**, 265 (1985).
- [29] M. D. Newton, Quantum chemical probes of electron-transfer kinetics: The nature of donor-acceptor interactions, *Chem. Rev.* **91**, 767 (1991).
- [30] P. Villarreal, S. Miret-Artés, O. Roncero, G. Delgado-Barrio, J. A. Beswick, N. Halberstadt, and R. D. Coalson, A wave packet Golden Rule treatment of vibrational predissociation, *J. Chem. Phys.* **94**, 4230 (1991).
- [31] O. Roncero, N. Halberstadt, and J. A. Beswick, A three-dimensional wave packet study of $\text{Ar} \cdots \text{I}_2(\text{B}) \rightarrow \text{Ar} + \text{I} + \text{I}$ electronic predissociation, *J. Chem. Phys.* **104**, 7554 (1996).
- [32] D. H. Zhang and J. Z. H. Zhang, Time-dependent treatment of vibrational predissociation within the golden rule approximation, *J. Chem. Phys.* **95**, 6449 (1991).
- [33] D. H. Zhang, J. Z. H. Zhang, and Z. Bačić, A time-dependent golden rule wave packet calculation for vibrational predissociation of D_2HF , *J. Chem. Phys.* **97**, 927 (1992).
- [34] F. A. Gianturco, T. Mukherjee, and P. Paoletti, Positron scattering from polar molecules: Rotovibrationally inelastic collisions with CO targets, *Phys. Rev. A* **56**, 3638 (1997).
- [35] F. A. Gianturco, T. Mukherjee, and A. Occhigrossi, Computing positron annihilation in polyatomic gases: An exploratory study, *Phys. Rev. A* **64**, 032715 (2001).
- [36] T. Nishimura and F. A. Gianturco, Vibrational excitation of methane by positron impact: Computed quantum dynamics and sensitivity tests, *Phys. Rev. A* **65**, 062703 (2002).
- [37] T. Nishimura and F. A. Gianturco, Virtual-State Formation in Positron Scattering from Vibrating Molecules: A Gateway to Annihilation Enhancement, *Phys. Rev. Lett.* **90**, 183201 (2003).
- [38] F. A. Gianturco, T. L. Gibson, P. Nichols, R. R. Lucchese, and T. Nishimura, Modeling dynamical correlation forces in low-energy positron scattering from polyatomic gaseous: A comparison for CH_4 , *Rad. Phys. Chem.* **68**, 673 (2003).
- [39] T. Nishimura and F. A. Gianturco, The scattering of positrons from CF_4 molecules at ultralow energies, *J. Phys. B* **37**, 215 (2004).
- [40] T. Nishimura and F. A. Gianturco, The dominant "heating" mode: Bending excitation of water molecules by low-energy positron impact, *Eur. Phys. J. D* **33**, 221 (2005).
- [41] T. Nishimura and F. A. Gianturco, Enhanced positron annihilation in small gaseous hydrocarbons: Threshold effects from symmetric C-H bond deformations, *Phys. Rev. A* **72**, 022706 (2005).
- [42] F. A. Gianturco, P. Nichols, T. L. Gibson, and R. R. Lucchese, Metastable trapping of low-energy positrons by cubane: A computational experiment, *Phys. Rev. A* **72**, 032724 (2005).
- [43] J. Franz and F. A. Gianturco, Low-energy positron scattering from DNA nucleobases: The effects from permanent dipoles, *Eur. Phys. J. D* **68**, 279 (2014).
- [44] F. Carelli, F. A. Gianturco, J. Franz, and M. Satta, A dipole-driven path for electron and positron attachments to gas-phase uracil and pyrimidine molecules: A quantum scattering analysis, *Eur. Phys. J. D* **69**, 143 (2015).
- [45] K. Fedus, J. Franz, and G. P. Karwasz, Positron scattering on molecular hydrogen: Analysis of experimental and theoretical uncertainties, *Phys. Rev. A* **91**, 062701 (2015).
- [46] F. A. Gianturco and R. R. Lucchese, Computational investigation of positron scattering from C_{60} , *Phys. Rev. A* **60**, 4567 (1999).
- [47] R. Carey, R. R. Lucchese, and F. A. Gianturco, Positron scattering from C_{20} , *Phys. Rev. A* **78**, 012706 (2008).
- [48] B. Barbiellini, M. J. Puska, T. Korhonen, A. Harju, T. Torsti, and R. M. Nieminen, Calculation of positron states and annihilation in solids: A density-gradient-correction scheme, *Phys. Rev. B* **53**, 16201 (1996).
- [49] J. Kuriplach and B. Barbiellini, Improved generalized gradient approximation for positron states in solids, *Phys. Rev. B* **89**, 155111 (2014).
- [50] M. J. Frisch *et al.*, *Gaussian 09, Revision D.01* (Gaussian, Inc., Wallingford, CT, 2009).
- [51] J. C. Light, I. P. Hamilton, and J. V. Lill, Generalized discrete variable approximation in quantum mechanics, *J. Chem. Phys.* **82**, 1400 (1985).
- [52] G. Nyman, Computational methods of quantum reaction dynamics, *Int. J. Quantum Chem.* **114**, 1183 (2014).
- [53] NIST Chemistry Webbook, <https://webbook.nist.gov/> (accessed 28 July 2021).

- [54] See Supplemental Material at <http://link.aps.org/supplemental/10.1103/PhysRevA.104.062807> for detailed numerical results calculated using different β values.
- [55] B. Barbiellini and J. Kuriplach, Proposed Parameter-Free Model for Interpreting the Measured Positron Annihilation Spectra of Materials using a Generalized Gradient Approximation, *Phys. Rev. Lett.* **114**, 147401 (2015).
- [56] National Institute of Standards and Technology, Computational Chemistry Comparison and Benchmark DataBase Release 20 (August 2020) Standard Reference Database 101, <https://cccbdb.nist.gov/> (accessed 28 July 2021).